Airfoil Pressure Prediction Based on Physics-Informed Deep Learning Approach

Li Jiazhe[1], Yang Yunjia[1] & Zhang Yufei[1]

[1] School of Aerospace Engineering, Tsinghua University, China

Abstract

Supercritical airfoils are widely used in large airliners, and their unique profile design enables the reduction of compressibility drag under transonic flight conditions while ensuring lift. The design of supercritical airfoils needs to consider the geometry, thickness, and flow field characteristics and performance under different operating conditions, which is difficult to design empirically, and therefore the construction of fast predictive agent models under different operating conditions and geometries is an effective tool for assist the design. Existing agent models constructed by traditional methods such as the kriging method do not perform well, while models constructed by purely data-driven methods that directly use deep learning models face generalization and interpretability problems. In this study, a physics-informed deep learning method is used to construct a variational autoencoder (VAE) for transfer learning. The deep neural network is embedded with transonic similarity law, which reduces the data required for the training of deep neural networks and improves the model generalization capability. The model can be used to further complete the optimization under multiple operating conditions and achieve the automatic optimal design of supercritical airfoils.

Keywords: Supercritical airfoil; Variational autoencoders; Physics informed; Transfer learning

1. General Introduction

Airliner is an important way of long-distance transportation, and its performance is directly related to economic benefits and flight safety. Typical commercial airliners have a cruise Mach number of 0.76~0.86 [1], which is typical of transonic flight. Although the influence of the transonic effect can be reduced by wing swept back and other methods, the wing surface still generates a supersonic region and the subsequent shock wave, which causes shock wave drag and shock-boundary layer interference. NASA engineer Whitcomb proposed the “Supercritical Airfoil” [2] in 1967, through careful geometrical design, to control the suction peak in the low-pressure region of the leading edge to weaken the shock wave, and to utilize the trailing edge loading to ensure sufficient lift coefficient, and finally to retard the drag increase of the airfoil with the increase of Mach number.

To realize the objectives of faster flight speed, longer range, and higher load capacity, and to improve the flight efficiency and safety of airliners, the aerodynamic design of the wing needs to meet the requirements of cruise lift coefficient, lift-to-drag ratio, etc., and to evaluate the performance of off design points at different Mach numbers in response to the requirements of the overall design of an aircraft. Although the influence of three-dimensional effects is very significant in the flow of 3D airfoils, and the pressure distributions at different spreading locations cannot be simply predicted from the 2D flow, it is still necessary to refer to the flow of equivalent 2D airfoils to carry out the aerodynamic design of wings, so that the spreading pressure distributions can be further considered to reduce the induced drag and the location of shock waves can be considered to minimize the transverse flow. Therefore, 2D airfoil design and flow prediction are the basis of aerodynamic design.

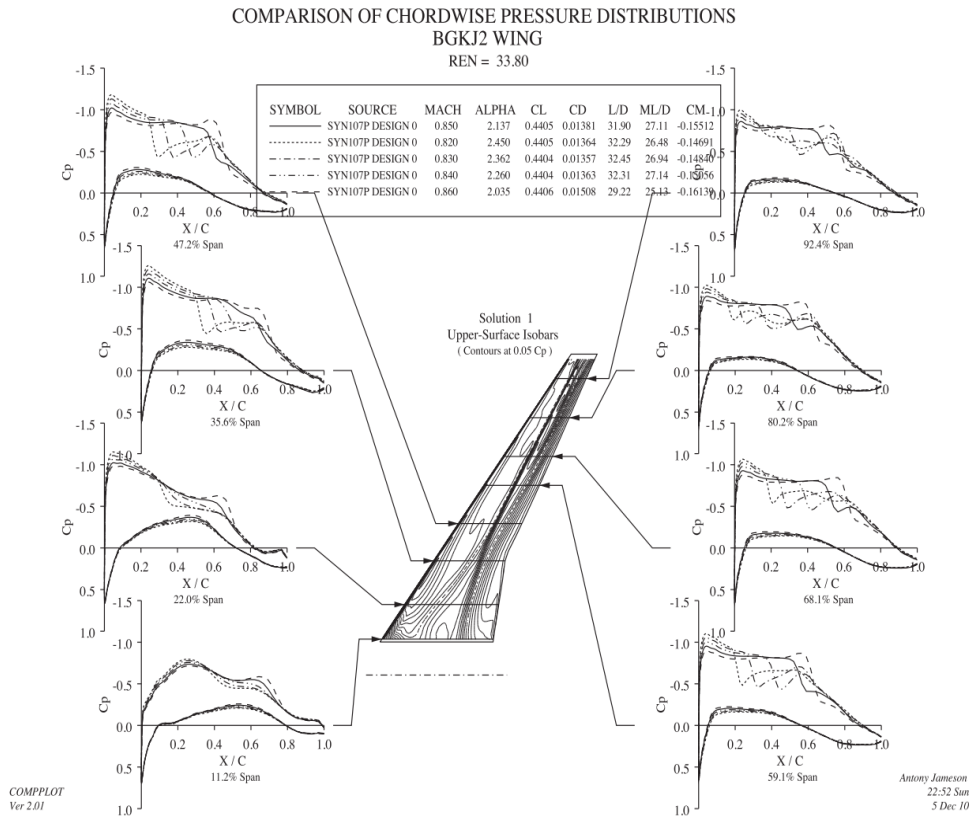

Figure 1 – Pressure distribution of an airfoil at different positions[4]

Traditional design methods have relied on aerodynamicists' insight into transonic flow phenomena. When numerical simulation methods and computational power were less developed in the last century, designers tended to rely on empirical rather than computational results. This design approach can be summarized as “design by trial and error”, where design metrics and flow structures are tuned based on simplified physical models and design experience. For example, Pearcy pointed out the critical wavefront Mach number to prevent shock-boundary layer separation [3], and the design criteria to control the pressure recovery altitude to prevent trailing edge separation, etc. These design experiences reveal the physical properties of the flow, and can inspire the designers to design the profiles while providing an intuitive understanding of the actual effects of the design parameters on the flow, and whether the design is robust or not. However, wing design as an “art” makes it difficult to realize the optimal “fine” design that satisfies each indicator's requirements, and the interference of a large number of design criteria also makes the design difficult. As airliners are updated and the design level increases, the experience needs to be updated in the face of more stringent aerodynamic performance requirements, safety, noise, and other constraints. These problems require fast and accurate methods for flow field prediction and performance evaluation.

With the increased accuracy and computational power of modern computational fluid dynamics (CFD) methods and advances in aerodynamic optimization methods, wing design has now gone from an “art” to a “science”. [4] With Computer-Aided Design (CAD) methods and highly accurate CFD techniques, designers can utilize flow data that “hides the physics of the flow” to directly compute the flow structure and performance for a given set of operating conditions and shape parameters and to combine with gradient optimization methods such as discrete adjoint methods [5] or global automatic optimization methods such as genetic algorithms [6], the optimal design can be carried out for quantifiable objectives. The emergence and advancement of these computational and design methods have greatly improved the design of airfoils. However, design methods combining CFD techniques and optimization algorithms still face problems such as large computation consumption and difficulty in coupling automatic optimization and design knowledge.

With the development of machine learning technology, there have been a large number of studies related to the use of machine learning technology to assist the design of aircraft. [7] Machine learning is a “computer program that learns from data” [8], which has been widely used in translation, search,

and other fields. The essence of machine learning is “representation learning”, which is used to obtain the distribution pattern of data; while deep learning “is a representation learning method with multi-level representations, which consists of simple but non-linear modules, each of which converts one level of representation (starting from the original input) into a higher, more abstract level of representation. abstraction-level representations. With enough combinations of such transformations, very complex features can be learned [9]."

Deep neural networks are realized by basic neurons spliced layer by layer for feed-forward inference, and their overall design form also determines how the model is used and characterized. A multilayer perceptron (MLP), which consists solely of multiple layers of neurons spliced together, is capable of realizing an output from an input that undergoes a nonlinear transformation. The autoencoder (AE) maps high-dimensional samples to low-dimensional “hidden variable” space by dimensionality reduction and dimensionality enhancement of the inputs, thus completing the information compression and feature extraction operations. Unlike principal component analysis (PCA) and other methods, the mapping method of AE to the low-dimensional space is automatic, nonlinear, and uninterpretable, so it is called an auto-encoder. The Variational Auto-Encoder (VAE) proposed by Kingma et al. in 2015 [10] adds a normal distribution in the latent space to the AE, constrains the distribution of the latent variables to be the multi-dimensional normal distribution, thus ensuring that the latent variables are well-distributed, and can randomly generate samples in the data distribution space by directly decoding the samples in the latent space.

Using different deep neural networks and training methods, deep neural networks have a wide range of applications in aerodynamic shape design. [11] For example, in geometric modeling, deep generative adversarial networks (GANs) are used to achieve parametric shape generation [19] and geometric filtering [12] for 3D airfoils to achieve the fast generation of effective geometric samples; in aerodynamic performance analysis and modeling, convolutional neural networks are used to predict lift coefficients [13][14] and construct agent models from design variables to performance metrics; For the direct prediction of the flow field, the flow field around a 2D airfoil is directly predicted based on convolutional networks [15] and U-net networks[16], and the downscaled model of the flow can also be obtained by using VAEs, etc., to realize the automatic generation of the real flow field[17]; for the optimization and design aided by machine learning, generative adversarial networks [18] or neural networks coupled with Gaussian process regression [19] are used for the aerodynamic optimization design of airfoils, etc. These methods model the geometry, flow field, and performance at different stages of the design, realizing the data-driven assisted design.

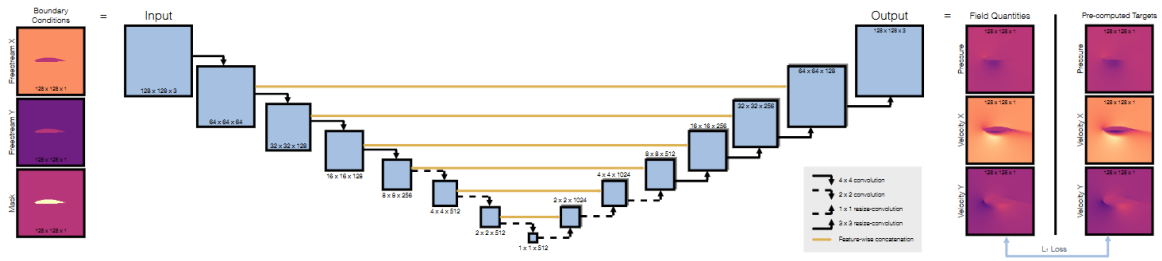

Figure 2 - Prediction of airfoil flow field based on U-net [16]

However, purely data-driven methods still face the problem of data shortage. For practical engineering problems, both high-precision CFD calculations and high-confidence experiments are expensive and time-consuming, and it is difficult to generate data in large quantities. The shortage of data leads to the fact that the neural network models for machine learning-assisted aerodynamic design are all “small models” with limited model generalization capability. The nature of purely data-driven agent models also dictates that “the model may fit observations well, but due to extrapolation or observational bias, the predictions may not match the actual situation or have low confidence, resulting in poor generalization performance”. [20]In addition, neural networks also face the problem of “hiding the physical flow principle”, and the results obtained from neural network prediction are only non-linear fits the data used in training, which not only makes it difficult to transfer and generalize the model, but also makes the model non-interpretable, and optimization and prediction based on the deep learning model are difficult to be understood and adopted by human experts. Optimization and prediction based on deep learning models are difficult to be understood and accepted by human

experts. In the face of these problems, a large number of studies in recent years have attempted to embed physical laws and design experience into deep learning models, so that the deep learning models partially satisfy the existing physical laws, and can have a certain degree of interpretability and generalizability.

Physics-inspired machine learning refers to “teaching” physical rules to machine learning models, “providing strong theoretical constraints and inductive biases based on observational a priori”[20]. Physics-inspired machine learning hopes to leverage pre-existing physical constraints (e.g., conservation of mass, etc.) and design experience to reduce the amount of data required or to improve the generalizability of neural networks. The most direct way of physical coupling is to directly utilize the control equations as loss functions for network training, i.e., the Physics-Informed Neural Network (PINN) proposed by Raissi et al [21]. This model achieves partial differential equation solving using neural networks by designing the inputs and outputs of the network as the independent and dependent variables of the partial differential equations and embedding the partial differential equations directly into the loss function as constraints.

However, although the idea of PINN is beautiful, PINN currently tends to have low accuracy or even fails to converge in complex problems, such as complex geometric problems. Therefore, introducing physical laws in traditional deep learning models in some ways is a feasible way of physical embedding. Specific implementations include introducing physical constraints to the loss function during machine learning training[22], introducing physical prior knowledge during model initialization[23], and hybrid machine learning models coupled with physical prediction models [24], among other methods. These physics-informed methods can enhance the accuracy of the model, and have a large number of applications in reduced-order modeling, turbulence modeling, uncertainty analysis, equation discovery, and data generation [25].

Overall, data-driven aerodynamic design can be carried out by utilizing the powerful nonlinear fitting ability of neural networks, constructing agent models and reduced-order models, etc. To solve the data shortage, generalizability, and interpretability problems brought by pure data-driven methods, there are a large number of researches to improve the training data, network structure, loss function, etc., and to couple the physical constraints and design experience with deep learning models. These studies bring inspiration for data-knowledge dual-driven aerodynamic design.

In this paper, we propose to construct a variational autoencoder network (VAE) to realize the fast prediction from the geometry of supercritical airfoils to the surface pressure distribution. The generalization performance and accuracy of the networks are improved by introducing the transonic similarity law, and the amount of data required for training is reduced. The research idea is as follows: firstly, the geometric family of supercritical airfoils that meets the requirements is generated based on the literature [26], and the CFD calculations of the flow field of transonic airfoil are carried out at the appropriate Mach number and thickness, and the geometric-airfoil surface pressure distributions are generated for the training of neural network; then, the VAE model is constructed based on the one-dimensional convolutional neural network and the multilayer perceptron to carry out the depth mapping from geometry to pressure distributions at a given Mach number. After obtaining the pretrained neural network, a transfer learning model is constructed and transfer learning is carried out at different Mach numbers, while the correction of transonic similarity law is carried out to compare the advantages of physics-informed methods. The model used in this paper is physically embedded based on the VAE model, which is innovative in neural network-assisted aerodynamic design. The overview of the research methodology is shown in Figure 3

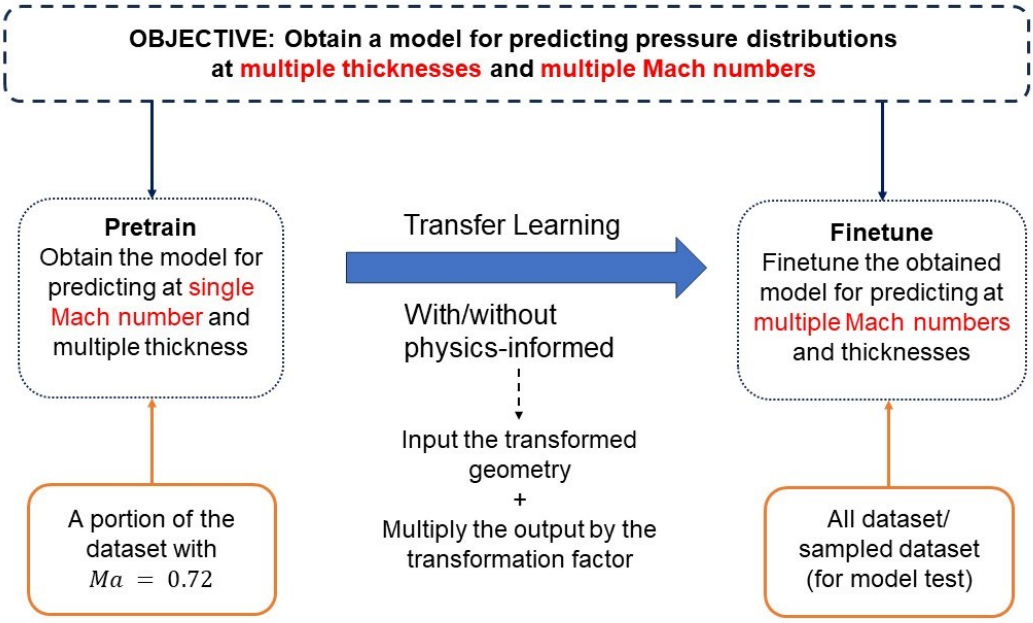

Figure 3 - Overview of the Methodology

The first chapter of the paper introduces the development and design of supercritical airfoils as well as the research progress in the field of deep learning-assisted aerodynamic design; the second chapter introduces the generation of the dataset; the third chapter introduces the network structure; the fourth chapter introduces the pretraining and transfer learning process and the advantage analysis of the physical embedding; and the fifth chapter carries out the summary and outlook of the research.

2. Generation of Datasets and Transonic Similarity Law

In this chapter, the mesh is automatically generated based on the supercritical airfoil geometry database, and the flow field data with different thicknesses and Mach numbers are obtained and post-processed to obtain a structured dataset for neural network training. The calculation results of the dataset are analyzed to validate the transonic similarity law and analyze the source and distribution of the error.

2.1 Mesh Generation and Calculation

The dataset generated in this study is based on NASA's open-source CFD calculation software CFL3D, and the numerical format and equation dimensionless processing used are described in its documentation. The turbulence model is the Mentor SST k-ω model [27], which is widely used for solving the flow of transonic airfoils with high accuracy and stability.

The geometry of supercritical airfoils has specific shapes to meet the design requirements of transonic airfoils, such as a flat suction plateau at the leading edge, a weak shock wave after the suction plateau, and a backward curvature of the trailing edge on the lower surface to reduce and then increase the pressure to cause after-loading, and so on. Therefore, the direct use of geometry-oriented parametric modeling methods (e.g., B-spline curves, etc.) will produce a large number of geometries that do not meet the requirements of supercritical airfoil design and cannot be directly used for neural network training. To address this problem, research [26] has ensured the reasonableness and unbiasedness of the airfoil pressure distribution by screening and sampling airfoils oriented to the Mach number distribution through the method of building an agent model with radial basis function response surfaces. The constrained Mach number distribution includes the leading-edge suction peak Mach number, the shock wave position, the Mach number before the shock wave, the highest Mach number on the lower surface, and the flatness of the suction

platform. The dataset used in this study was generated based on this approach and contains 1420 supercritical airfoil geometries.

The geometry parameterization is based on the CST method [28] and is represented using 10th-order Bernstein polynomials to ensure modeling accuracy. After obtaining the geometry, the initial C-mesh is established by direct interpolation, and the boundary layer encryption and mesh orthogonalization are adjusted using elliptic iteration.

The physics-informed model constructed in this study utilizes the transonic similarity law transform to map the pressure distributions of airfoils at different Mach numbers to the same Mach number by varying the thickness, thus requiring training at only a single Mach number and fast transfer training at different Mach numbers. The similar parameters derived from the transonic similarity law have a corresponding decrease in thickness for increasing Mach number, as shown in Figure 4. For the model to obtain the ability to correct the pressure distribution after the transformation of the transonic similarity law during the subsequent transfer training, the thickness corresponding to the same similar parameter needs to be calculated at different Mach numbers, i.e., the distribution range of the thickness is different at different Mach numbers.

In addition, the derivation of the transonic similarity law is carried out in the "wind-axis system", i.e., the angle of attack of the incoming flow is 0°. To comply with the assumption of the transonic similarity law and to facilitate subsequent training, a tensile transformation is required in the vertical incoming flow direction, and the angle of attack needs to be changed simultaneously when generating airfoils of different thicknesses. For each airfoil geometry, Mach numbers 0.70, 0.72, and 0.74 were taken, and three thicknesses of 0.09, 0.1, and 0.11 were taken at Mach number 0.72 for training the model at constant Mach number. For the other two Mach numbers the corresponding thicknesses were calculated based on the similar parameters of 2.2 and the angle of approach settings were transformed, and the combined geometric and computational parameters are shown in Table 1. The Reynolds number was calculated to be 2×10^7, and a total of 12,780 flow fields were constructed and the geometric coordinates and pressure coefficients at 600 points on the surface were extracted to obtain the dataset for training.

Table 1 - Settings of Dataset

Mach	thickness/ AoA (1)	thickness/ AoA (2)	thickness/ AoA (3)
0.70	0.104/ 3.11°	0.115/ 3.46°	0.127/ 3.81°
0.72	0.090/ 2.70°	0.100/ 3.00°	0.110/ 3.30°
0.74	0.078/ 2.33°	0.086/ 2.56°	0.095/ 2.84°

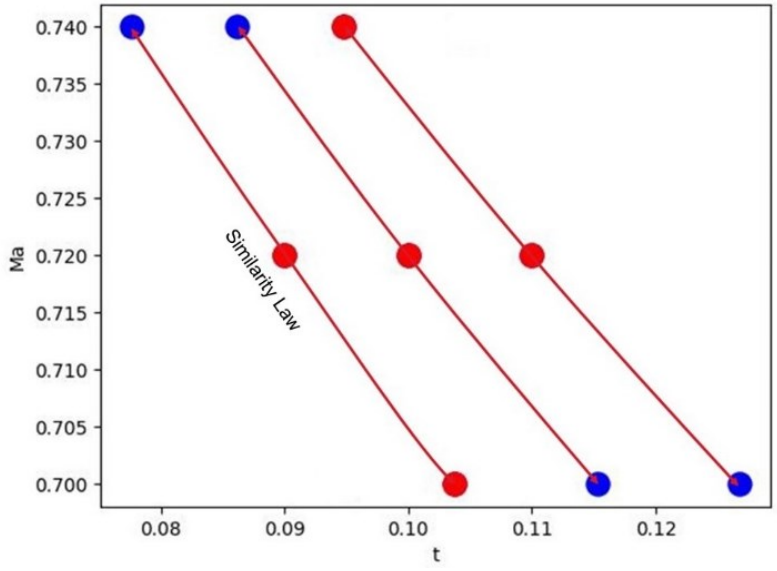

Figure 4 - Settings of Dataset

Figure 5 illustrates the change in pressure distribution pattern for a typical supercritical airfoil thickness change, where the pressure is dimensionless in the following manner:

$$P = \frac{\tilde{p}}{\widetilde{\rho_\infty}(\widetilde{a_\infty})^2} \tag{1}$$

It is obvious that the far-field pressure $p_\infty = \frac{1}{\gamma}$.

The overall curvature of the airfoil increases when the thickness increases, which is manifested in the lower surface as a decrease in the lowest pressure coefficient and thus an increase in the absolute value of the overall pressure gradient, and the upper surface as a decrease in the pressure coefficient of the suction platform, a delay in the location of the shock wave, and an increase in the gradient of the pressure recovery after shock wave.

2.2 Transonic similarity law and verification

The transonic similarity law is a law derived from aerodynamics based on the velocity-potential equation and small perturbation theory, which describes the similar characteristics of the pressure distribution of a thin wing across the speed of sound. For adiabatic, spinless flow, the following velocity-potential equation is available:

$$(a^2 - u^2)\frac{\partial u}{\partial x} + (a^2 - v^2)\frac{\partial v}{\partial x} + (a^2 - w^2)\frac{\partial w}{\partial x} = uv\left(\frac{\partial u}{\partial y} + \frac{\partial v}{\partial x}\right) + vw\left(\frac{\partial v}{\partial z} + \frac{\partial w}{\partial y}\right) + uw\left(\frac{\partial u}{\partial z} + \frac{\partial w}{\partial x}\right) \tag{2}$$

Substituting the small perturbation assumption:

$$u = V_\infty + u', v = v', w = w' \tag{3}$$

and coupled with an expression for the speed of sound given by the energy equation:

$$a^2 = a_\infty^2 - \frac{\gamma - 1}{2}\left(2V_\infty u' + u'^2 + v'^2 + w'^2\right) \tag{4}$$

After neglecting second-order small quantities, the transonic small perturbation equation is obtained:

$$(1 - Ma_\infty^2)\frac{\partial u}{\partial x} + \frac{\partial v}{\partial y} + \frac{\partial w}{\partial z} = Ma_\infty^2(\gamma + 1)\frac{u}{V_\infty}\frac{\partial u}{\partial x} \tag{5}$$

Replacing the velocity potential in the two-dimensional case is expressed as:

$$\frac{\partial^2 \phi}{\partial x^2} + \frac{1}{1 - Ma_\infty^2}\frac{\partial^2 \phi}{\partial y^2} = \frac{(\gamma + 1)Ma_\infty^2}{1 - Ma_\infty^2}\frac{1}{V_\infty}\frac{\partial \phi}{\partial x}\frac{\partial^2 \phi}{\partial x^2} \tag{6}$$

Similar parameters are obtained:

$$K = \frac{1 - Ma_\infty^2}{\left((\gamma + 1)Ma_\infty^2\right)^{\frac{2}{3}}\bar{b}^{\frac{2}{3}}} \tag{7}$$

A similar relationship for the pressure distribution can be obtained from the expression for the wall pressure distribution coefficient:

$$C_p = -\left(\frac{\bar{b}^2}{(\gamma + 1)Ma_\infty^2}\right)^{\frac{1}{3}} P(K, \bar{x}, \bar{y}) \tag{8}$$

Therefore, the pressure distribution is similar for cases with the same similarity parameter, and if the similarity law is to be used it is necessary to control the airfoil geometry and the similarity parameter K to be the same. The form of the similarity parameter suggests that the similar airfoil thickness decreases as the incoming Mach number is less than 1, which is under the same law of decreasing pressure gradient at the lower surface that is satisfied when the Mach number increases and the airfoil thickness decreases.

At the same time, the above derivation also shows that the transonic similarity law assumes that the flow is isentropic and the airfoil is thinner. However, the actual working conditions (and the dataset constructed in this study) are viscous and contain shock waves, the flow is not isentropic, and the airfoil has a certain thickness, which leads to some errors in the application of the similarity law, and therefore need to be corrected in the transfer learning.

Application and validation of the similarity law. The dataset generated in 2.2 has been considered to

maintain the same similarity parameters at different Mach numbers, and the results are shown in Figure 6, where the pressure coefficient curves for Mach numbers 0.70 and 0.74 have been corrected by the coefficients in Eq. (9). It can be seen that the direct prediction given by the transonic similarity law is more accurate before and after the shock wave and on the lower surface of the airfoil, but the pressure distribution at the location of the shock wave and a short section after the shock wave are not accurate. This result is consistent with the assumption made in the derivation of the transonic similarity law, which can be regarded as approximately isentropic before the appearance of the shock wave, while there is a significant entropy increase after the appearance of the shock wave, so the similarity does not hold. This error should be compensated by the neural network.

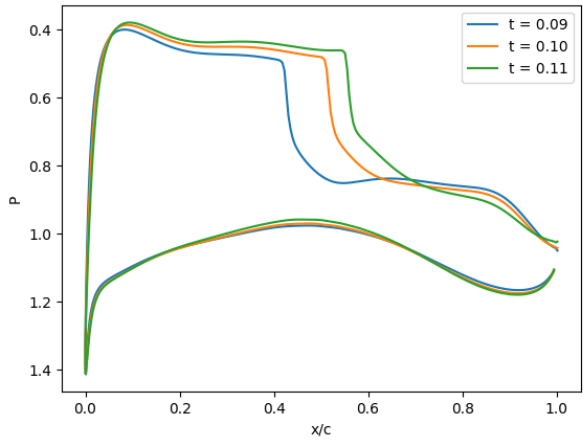

Figure 5 - Pressure distribution of supercritical airfoils with different thicknesses

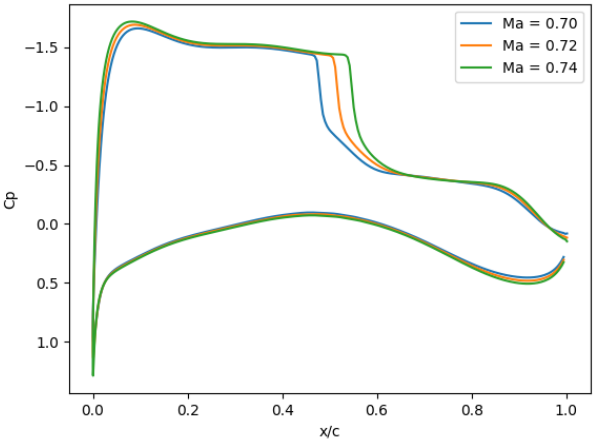

Figure 6 - Verification of the transonic similarity law

3. Structure of the Proposed Model

3.1 VAE Structure

Through the stitching of the base model, a model that meets the input and output requirements can be constructed to build a surrogate model. A straightforward idea is to input the airfoil geometry and quickly derive its surface pressure distribution from the surrogate model. Based on this idea, a variational autoencoder model (VAE) can be constructed, which is based on the autoencoder (AE) and consists of an encoder and a decoder, as shown in Figure 7. Although the geometry and pressure distribution of the airfoil are high-dimensional data (equal to the number of mesh points on the airfoil surface during the calculation), they are in essence low-dimensional manifolds in a high-dimensional space, and the AE automatically extracts the "latent variables" (characteristic variables)

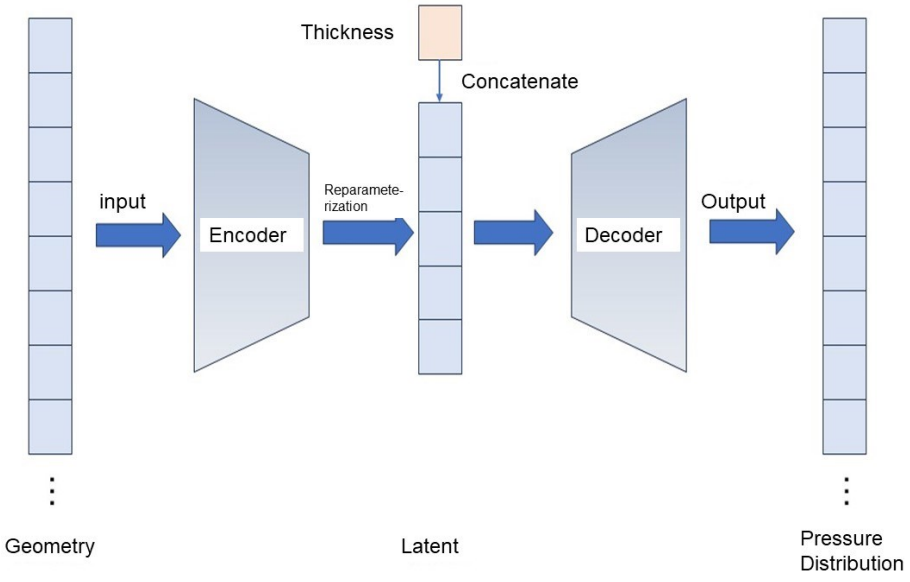

Figure 7 - Structure of VAE

of the airfoil geometry-pressure distribution data, which means that the high-dimensional geometric data are transformed into the low-dimensional hidden variables by the nonlinear encoder and can be used by the decoder. In other words, the high-dimensional geometric data are transformed into low-dimensional latent variables by a nonlinear encoder, and the pressure distribution is reconstructed from the hidden variables by a decoder.

Due to the sparsity of high-dimensional space, the hidden variables are prone to discontinuous distribution in physical space, i.e., when changing a certain physical quantity of input, the hidden variables change drastically, which leads to the output data not being robust (poor generalization); some parts of the space of the latent variables may not correspond to the physical input data, i.e., the "posterior distribution" of the output data obtained by sampling the hidden variables is not correct. On the other hand, the distribution in the physical world is generally normal, i.e., most of the data are distributed around the "mean", and the further away from the mean the rarer the data are. To achieve a "better" distribution in the hidden variable space, constraints can be added to make the hidden variables "normally distributed" in the distribution of the input dataset, so that the wing pattern that meets the requirements can be obtained directly by sampling the hidden variables, and the neural network-based feature extraction can be realized. The specific form of the constraint is described in detail in Section 4.1, which is expressed in the network structure by outputting the mean μ and variance σ of the hidden variables from the decoder, and then sampling ε from the standard normal distribution N(0, I), and combining them to obtain the hidden variables:

$$z = \mu + \sigma \bullet \varepsilon \tag{9}$$

The encoder and decoder can have different forms, since the airfoil geometry and pressure distribution are both high-dimensional structured data, a one-dimensional convolutional network is chosen as the encoder and decoder in this study, and the data characteristics of each layer of the encoder are shown in Table 2. Each layer of the decoder adopts inverse convolution, i.e., upsampling first and then doing convolution in reverse to realize the stride operation in convolution, and the shape of the output data of each layer corresponds to that of the encoder.

Table 2 - Hyperparameters of Encoder

Layers	Hyper-Parameters	Tensor Shape
1	Dims=64, Stride=2, Padding=1	64×150
2	Dims=64, Stride=2, Padding=1	64×75
3	Dims=128, Stride=1, Padding=1	128×75
4	Dims=128, Stride=2, Padding=1	128×38
5	Dims=128, Stride=2, Padding=1	128×19
6	Dims=256, Stride=1, Padding=1	256×19
7	Dims=256, Stride=2, Padding=1	256×10
8	Dims=256, Stride=2, Padding=1	256×5
9	MLP（input 1280，output 20）	20

3.2 The Model for Physics-Informed Transfer Learning

Transfer learning refers to the use of an already trained model for further training on a new dataset. In the process of transfer learning, a module is generally spliced after the output layer of the model as a transformation of the model's output to a dataset with a different distribution. The output of the model in this study is a high-dimensional pressure distribution, for which the transformation is more difficult to train and more parameters are added. Since the VAE has automatically extracted the high-dimensional distribution features of the dataset to the low-dimensional latent variable space, a nonlinear transformation of the latent variables will be performed to achieve the purpose of transfer learning. The specific structure is shown in Figure 8, in which the transfer layer is a new structure, which consists of four layers of MLP to form the residual structure and is used to learn the

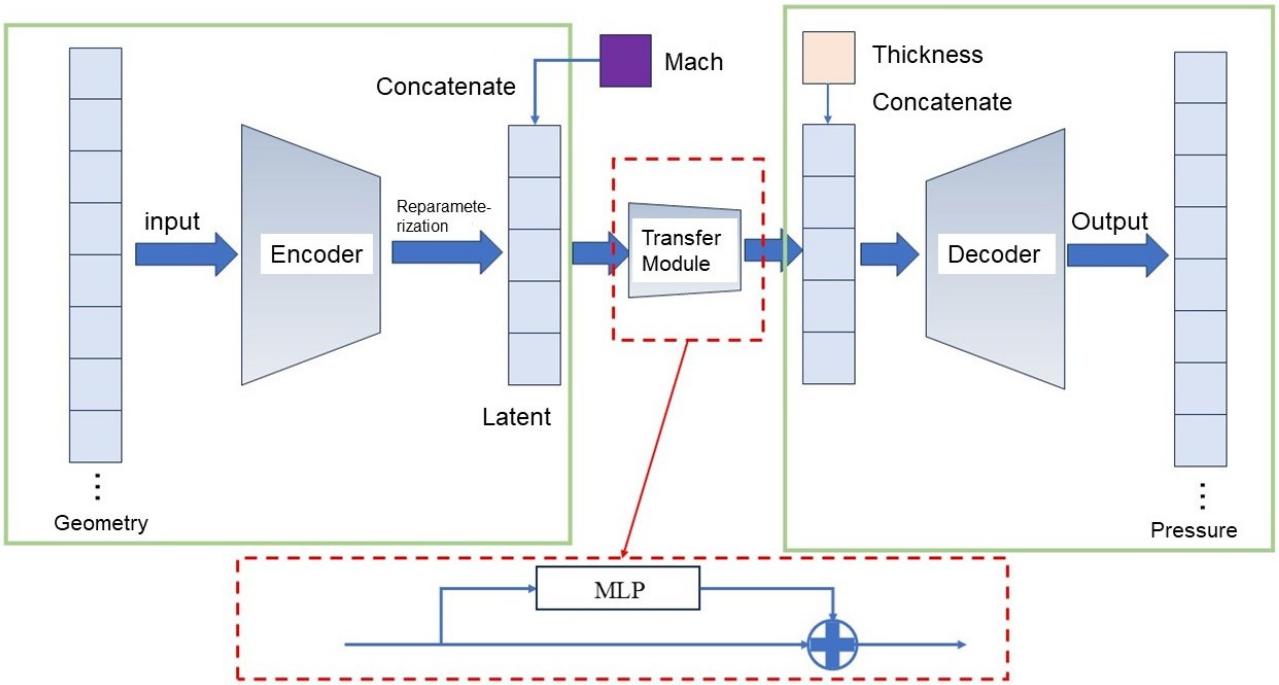

Figure 8 - Models for Transfer Learning

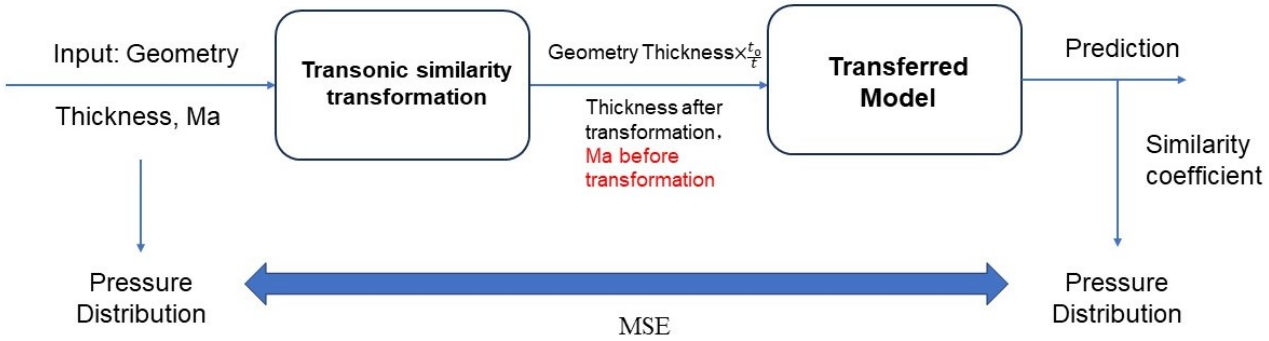

Figure 9 - Physics-Informed method

differences of the latent variables under different Mach numbers by nonlinear mapping of the latent variables spliced with Mach numbers.

To embed the physical law of transonic similarity in the model, the network inference method shown in Figure 9 was designed. Although this inference method is a transformation-based computational method, the model using the physics-informed method can be referred to as a "physics-informed model" because the parameter transformations are performed in the model and the outputs are corrected by transfer training the already pre-trained model.

When the model is trained, backpropagation is used to derive the derivatives of each parameter of the model concerning the Loss function and perform gradient descent. When transfer learning, the parameters of other modules can be fixed to train the transfer layer alone, in such a way that the backward derivation can be cut off behind the modules that do not need to be trained, reducing the time and memory consumption required for backpropagation; or the parameters of all modules can be trained to fine-tune the parameters, and the original model is only given as initial parameters for training. In the next chapter, we will test and analyze the characteristics and network performance of the two training methods, for the sake of narration, the model that fixes some parameters is called the "frozen model", while the model that trains all parameters is called the "non-frozen model".

4. Model Training and Physics-Informed Test

In this chapter, we use the dataset generated in Chapter 2 with only Ma=0.72 for each airfoil pressure distribution to pretrain the model first. Each airfoil contains three types of thicknesses, thus a total of 4260 airfoil-pressure distribution data is used. The pre-trained network is used to further

obtain the network that can be used for predicting supercritical airfoil pressure distributions at different Mach numbers and different thicknesses in 4.2 by the physics-informed transfer learning.

4.1 VAE pretraining test

The standard VAE network is first trained, with the parameters described in 3.2 and a total number of parameters of 1341545. The model inputs the geometry of the airfoil and outputs the pressure distribution corresponding to that geometry for a specific operating condition.

The loss function is used for training:

$$Loss_{VAE} = Loss_{MSE} + \alpha_{KL} Loss_{KL} \tag{10}$$

α_{KL} is the coefficient to balance the two weights. Assuming that the amount of data in each batch of training is b, and the number of sampling points for each geometric and pressure distribution is p, then:

$$Loss_{MSE} = \sum_{i=1}^{b} \sum_{j=1}^{p} \left(P_{recons;i,j} - P_{real;i,j}\right)^2 \tag{11}$$

Assuming also that the latent variable dimension is d_h, then:

$$Loss_{KL} = -\frac{1}{2} \sum_{i=1}^{d_h} \left[2log\sigma_i + 1 - \sigma_i^2 - \mu_i^2\right] \tag{12}$$

In practice, since the neural network output value has positive and negative, $log\sigma_i{}^2$and μ_i are used as the output of the encoder.

The training parameters are as follows: the amount of data in each batch (Batch Size) is 32, the training batch (Epoch) is 1000, the latent variable dimension (Latent Dimension) is 20, the KL loss term weight$\alpha_{KL} = 1 \times 10^{-5}$, and the training is carried out by using Adam's optimizer with an initial learning rate of 1×10^{-4}. The training process loss decline curve is shown in Figure 10. All subsequent plots of Loss decline with Epoch have the vertical coordinates as the logarithm of the actual Loss in (10) with base 10.

The model prediction results are shown in Figure 11, which shows that the model predicts better for the more typical pressure distribution patterns (a, b, c), while the prediction error increases for the individuals with more forward shock wave positions and irregular suction platforms (d, e, f), but still captures the pressure distribution patterns at the shock wave positions and after the waves well. This indicates that the VAE model can infer the pressure distribution based on the geometry of the airfoil. The VAE model finally has an MSE of 1.1×10^{-4} in the test set.

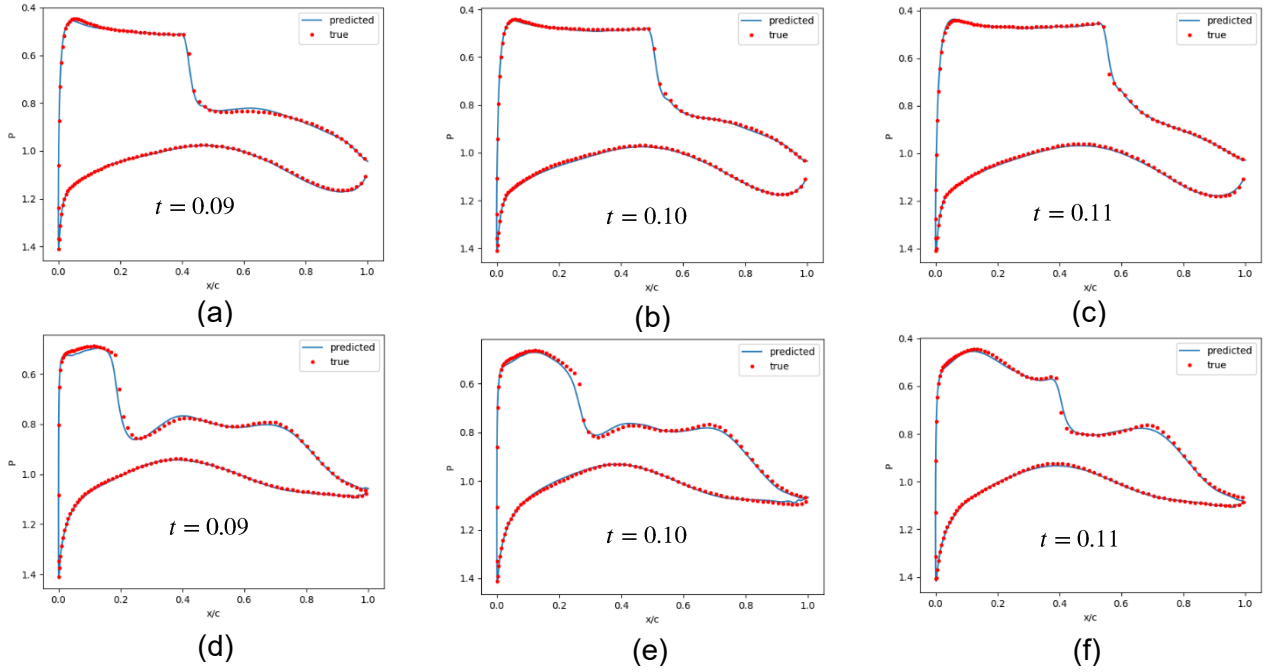

Figure 11 - Prediction Result of the VAE model

The VAE network was tested for extrapolated predictions, i.e. the model was used to predict the pressure distributions for two cases of thicknesses of 0.08, and 0.12, respectively, on the same airfoil, which were outside of the thickness range of the training dataset. The prediction results are shown in Figure 12. It is obvious that the model prediction accuracy is significantly lower than that of the interpolation, but it can still predict the location of the shock wave, the location of the suction platform, and the pressure on the lower surface after the thickness change more accurately, while the prediction after the shock wave is less accurate. This may be because the shock wave is a strongly nonlinear structure and contains unequal entropy physical features that cause changes in the pressure distribution pattern that generate new properties when the thickness changes significantly, thus exceeding the predictive ability of the model.

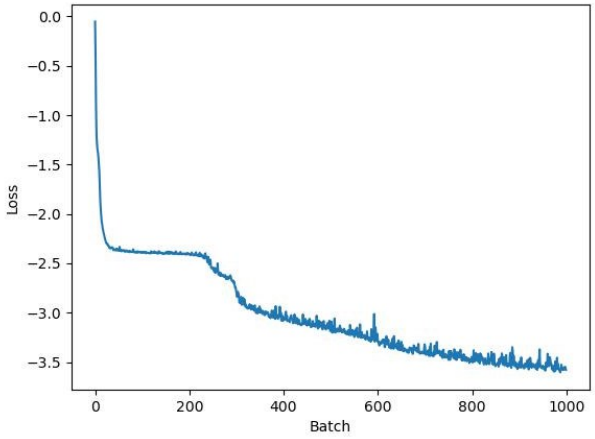

Figure 10 - VAE Network Training Loss Descent Curve

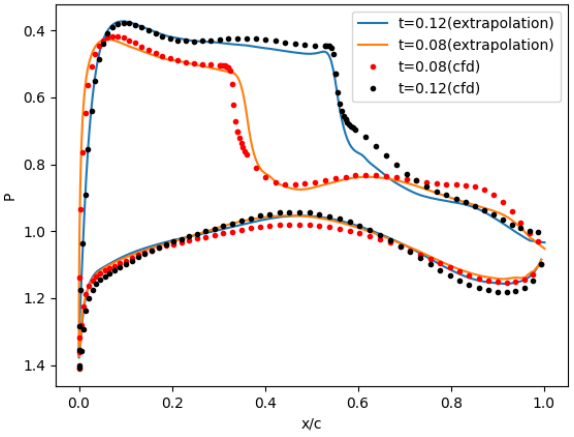

Figure 12 - Extrapolation result for VAE

4.2 Physics-Informed Transfer Learning

Using the VAE model at a constant Mach number obtained in 4.1, the physical properties of the transonic similarity law are coupled for transfer learning at different Mach numbers.

The transfer model is trained using the Adam optimizer with a constant learning rate of 0.0001. The first full-sample transfer learning training is performed, and the loss decline curve of the training process is shown in Figure 13, in which the results of training only the transfer layer with the rest of the parameters fixed have converged (the loss is no longer decreasing) at about 400 Epochs; while the results of training all the parameters have been decreasing in the training process at 1,000 Epochs. The error has been decreasing during the training process of 1000 Epochs.

The models obtained from the two training methods were tested with mean squared errors of 1.52×10^{-4} and 8.99×10^{-5} on the test dataset, and the prediction results are shown in Figure 14. The lines in the figure show the output of the model predictions, and the dots are the results of the

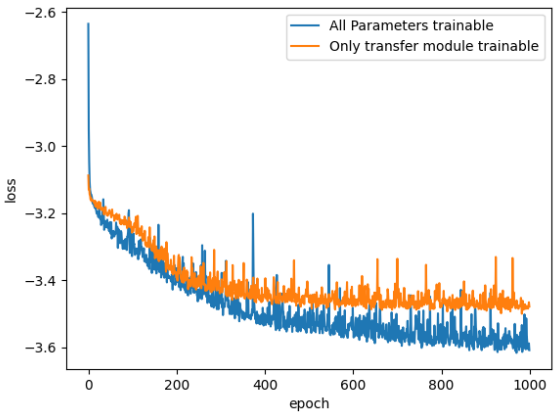

Figure 13 - Loss curves for the training process of physics-informed transfer learning

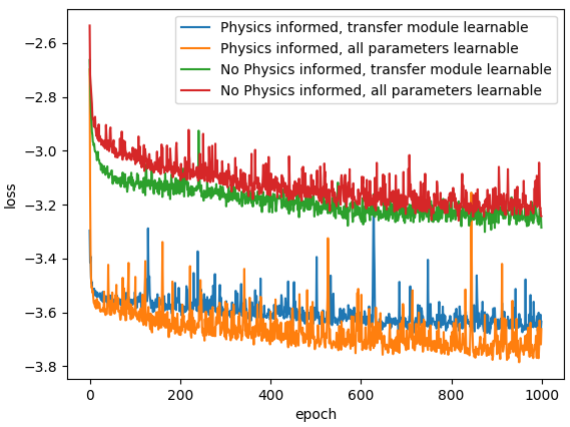

Figure 16 - Decline curve of training loss for small samples

CFD calculations. (a), (b), and (c) are the results of training only the transfer layer with Ma = 0.70, Ma = 0.72, and Ma = 0.74, respectively, whereas the remaining three figures are the results of the full parameter training fine-tuning. Both in terms of the mean error and the accuracy of the predictions in the plots, all-parameter fine-tuning outperforms training the transfer layer only. This result is to be expected since training only the transfer layer makes the model constrained with the original parameters and the representation ability is weaker than training all parameters directly.

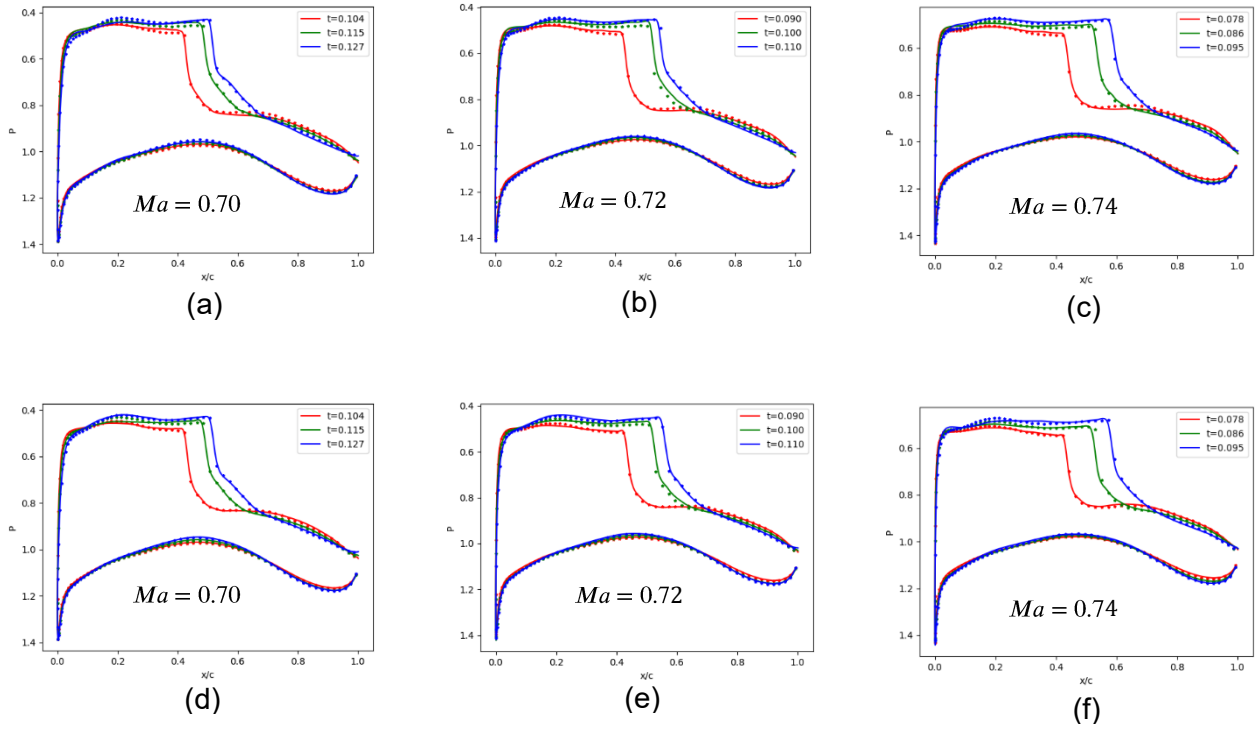

Figure 14 - Prediction results of the physics-informed model

The goal of transfer learning is to obtain a model that can accurately predict the target space using a small number of samples from the target working conditions for fast training. To test this capability, in this subsection, an attempt is made to train the model with only one thickness of the airfoil selected for each of the two working conditions at Mach numbers of 0.70, and 0.74, as shown in Figure 15. To prevent the performance of the model from degrading under the original operating conditions, the data of the original Mach number 0.72 is added to the training set. The transformation of the similarity law makes the thickness of the airfoil with similar pressure distribution decrease when the Mach number increases, and the original model is trained with a thickness range of 0.09~0.11 at Mach number 0.72, then the model embedded with the transonic similarity law is shifted from the allowed thickness range of 0.09~0.11 during the transformation. To compare the performance of the physics-informed model and the direct transfer learning model, the data with both the original thickness and the transformed thickness in the range of 0.09~0.11 are selected as the training set, i.e., they are the Mach number and the thickness represented by the red dots in the figure. One thickness each is additionally selected at Mach numbers 0.74 and 0.70 for the performance test of the direct transfer model, as shown by the green dots in the figure. The remaining blue dots serve as performance test data for the physics-informed model.

Training is performed on the training set shown in Figure 15, and the loss curves for different training methods are shown in Figure 16. With or without physics informed, the loss drop of transfer training is small, but the error at the beginning of the training of the physics-informed model is about 0.5 orders of magnitude lower compared to the direct transfer, which makes the prediction accuracy of the final physics-informed model under the training condition significantly higher than that of the model without physics-informed.

From the analysis in Section 4.1, the method of training all parameters of the model simultaneously yields better model performance, so the following compares the test performance of the model with

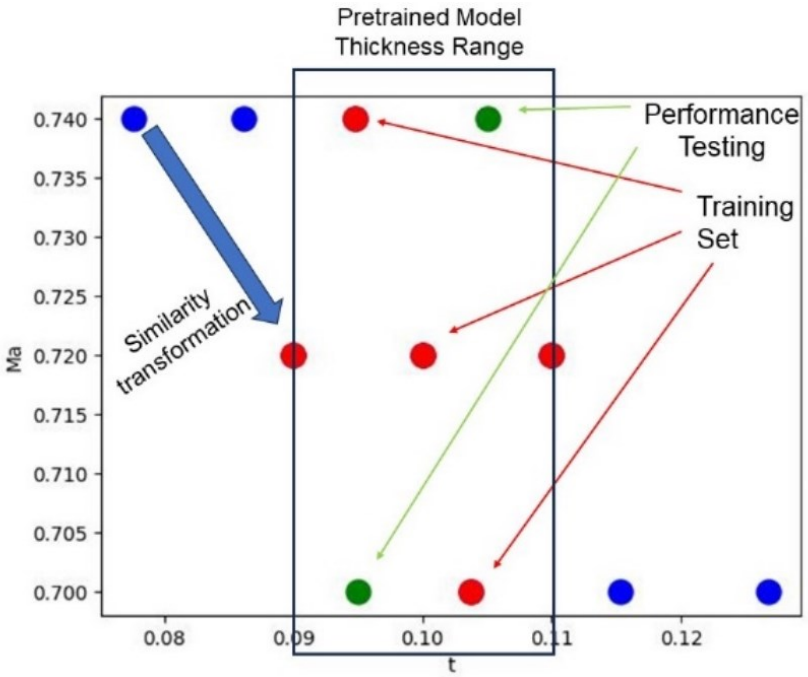

Figure 15 - Setup of small sample transfer training dataset

or without physics-informed in this way over the thickness and Mach number of the training set

The predicted results are shown in Figure 17. The lines in the figure show the output of the model predictions and the dots are the results of the CFD calculations. (a), (b), and (c) are the results for the physics-informed model and Ma = 0.70, Ma = 0.72, and Ma = 0.74, respectively, while the remaining three plots are the results for the non-physics-informed (direct training). The physics-informed model can make more accurate predictions on other thicknesses of the airfoil when trained with only one thickness, and although there are some errors, the trends of the shock wave location and the pressure of the low-pressure region are correct, while the directly trained model is unable to predict the pressure distribution correctly at all on the remaining thicknesses, except for the thicknesses that are accurately predicted by the trained model. It shows that the direct training model cannot predict untrained Mach number and thickness.

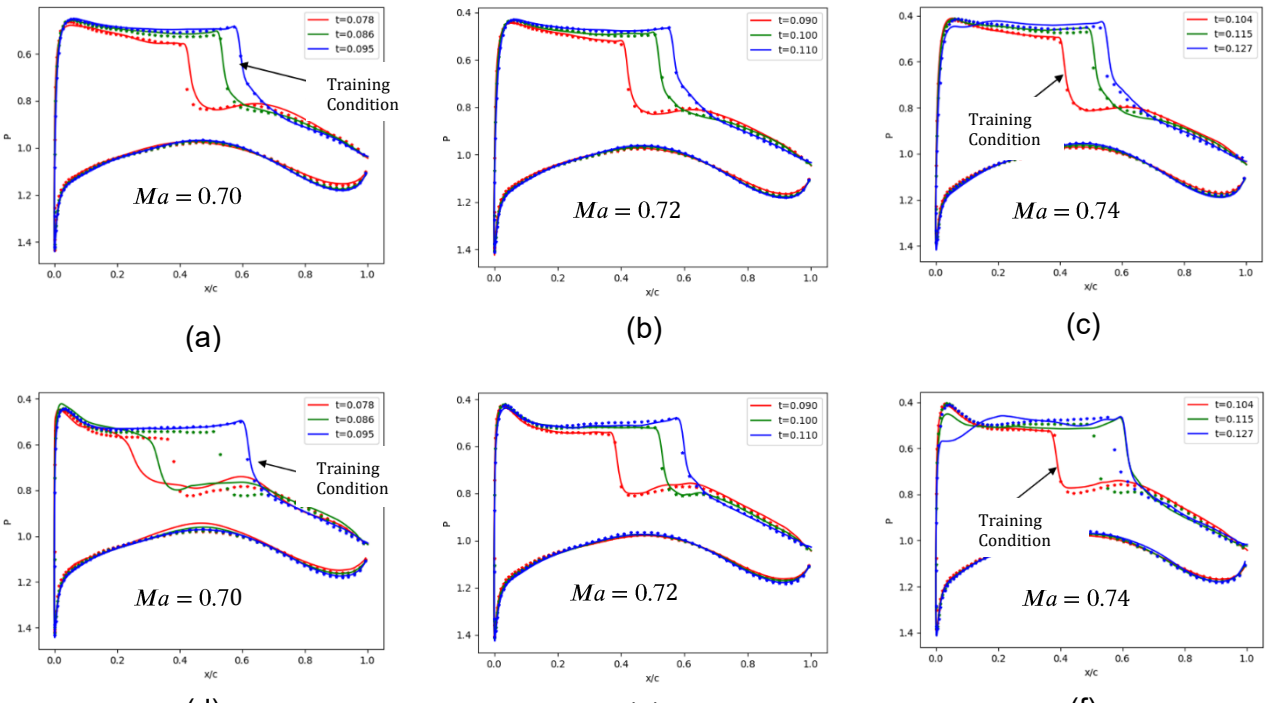

Figure 17 - Prediction results of models trained with small sampled dataset (under training conditions)

The thickness of the original model is 0.09~0.11, and the thickness of the model embedded in the transonic transformation can still be maintained at 0.09~0.11 at different Mach numbers after the transformation, while the direct training model is not transformed, and the thickness of the untrained case in Figure 17 is outside the range of 0.09~0.11, which belongs to the thickness of the "extrapolation". To exclude the influence of the performance degradation caused by the extrapolation, as shown in Figure 18, the test is carried out in the two cases of Ma=0.74,t=0.105 and Ma=0.70,t=0.095, and at this time, the physics-informed model (a, c) is equivalent to the thickness of the generalization, but the location of the shock wave and the height of the low-pressure region are more accurate, which indicates that the physics-informed model can maintain the generalization ability over thickness to some extent. In contrast, the input thicknesses of the directly trained models (b, d) are within the thickness range of the fixed Mach number training, but the shock wave positions are completely incorrect. The directly trained model did not gain the ability to predict over different Mach numbers.

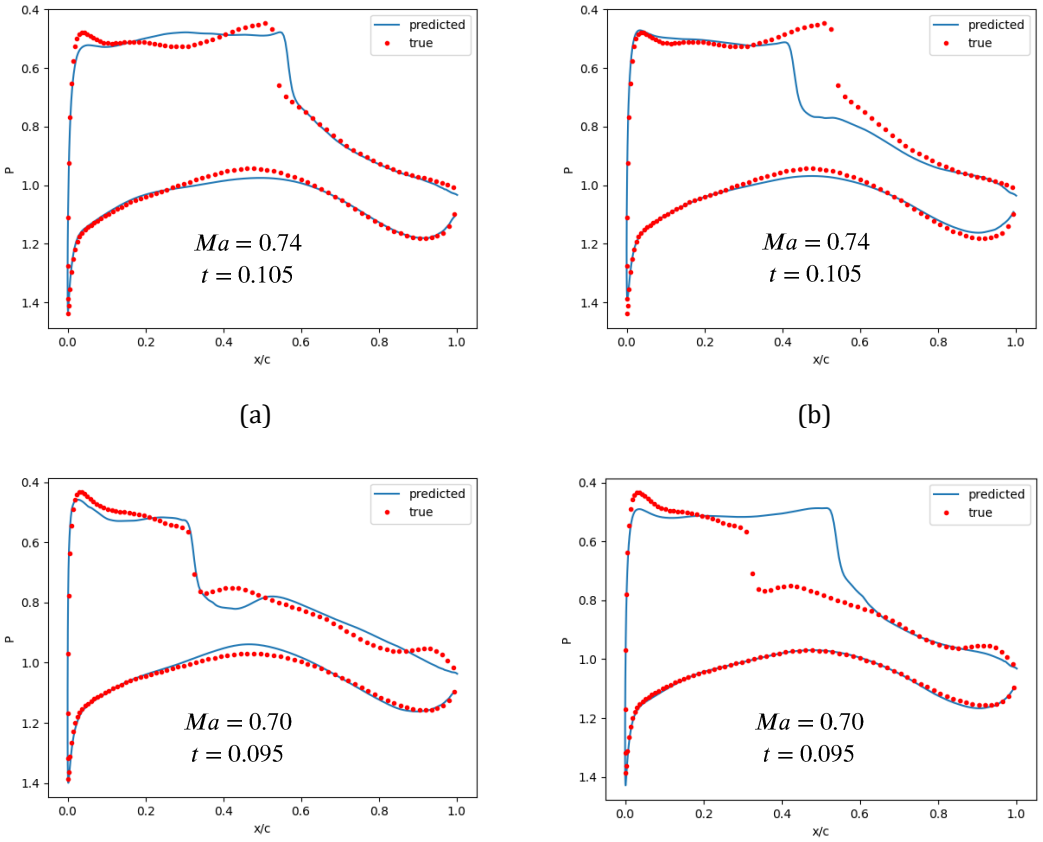

Figure 18 - Small-sample training model prediction effects (interpolated working conditions for direct training models and extrapolated for physics-informed model)

5. Summary

After the above analysis, the training obtains the VAE model coupled with the transonic similarity law, which can predict the supercritical airfoil pressure distribution in different Mach number and thickness for the prediction of supercritical airfoil pressure distribution; then, the study conducted the test of small-sample transfer learning, and the physics-informed model was able to utilize a small number of samples to obtain the prediction ability at different Mach numbers, while the model with direct transfer learning was unable to obtain the generalization ability, which verified the effect of physics-informed method.

There is still something to be further explored in the future. For example, this study only constructed multi-thickness data for training physics-informed models at different Mach numbers, and the model without embedded transonic similarity law only tested the small-sample learning capability with a single thickness. In the future, datasets containing multiple thicknesses at different Mach numbers

could be constructed for training the model without physics-informed, and the performance of the direct transfer model trained with a large amount of data could be tested and compared with the physics-informed model.

In addition, this study only tested the effect of the physics-informed method in model training, using a dataset computed at a fixed angle of attack, the model cannot predict at different angles of attack, so it is possible to construct a multi-angle of attack dataset, introduce the input module of the angle of attack in the model to establish a multi-angle of attack prediction model, and complete the aerodynamic optimization design based on the prediction model, or even the design of a three-dimensional airfoil.

In the study, it is found that the embedding of the transonic similarity law enables the model to have strong generalization and small-sample learning ability, however, there are still many issues worth exploring for the relationship between the physical law and the training data. For example, the error of the transonic similarity law is large for data with incomplete convergence using sparse grids or CFD computational iterations; does the embedding of the physical law still serve to enhance generalization and reduce the number of learning samples in this case? More generally, can the embedding of other physical laws, such as the embedding of mass conservation equations in two-dimensional flow field prediction, have the same effect? As well as whether the advantage of physics physics-informed method is related to the structure of the model, can the same conclusion still be obtained by replacing the VAE model with other types of networks (e.g., Transformer, etc.)? Subsequent research could therefore also fully explore the relationship between data-driven and knowledge-driven in this problem, guiding other aerodynamic and fluid mechanics knowledge-informed methods.

Overall, this study provides a feasible way to utilize physical laws to enhance model interpretability and generalization and reduce the amount of data required for training, and a comparison between physics-informed and non-physics-informed models is conducted to validate the advantages of the physics-informed approach. This approach is expected to assist various types of deep learning problems that contain rich physical laws and have practical applications in the construction of larger-scale aerodynamic agent models, such as the construction of wing pressure prediction models using three-dimensional swept-back theory.

Contact Author Email Address

Li Jiazhe: 1336882402@qq.com

Copyright Statement

References

[1] Sforza, Pasquale M. *Commercial Airplane Design Principles*. 1st edition, Elsevier, 2014.

[2] Whitcomb, Richard T. Review of NASA Supercritical Airfoils. *International Council of the Aeronautical Sciences Congress*, Israel, Haifa, no. ICAS PAPER 74-10, 1974.

[3] Pearcey, H. H. Some Effects of Shock-Induced Separation of Turbulent Boundary Layers in Transonic Flow Past Aerofoils. *Reports and Memoranda*, Vol. 23, No. 9, pp 1-61, 1955.

[4] Jameson, Antony, and Kui Ou. 50 Years of Transonic Aircraft Design. *Progress in Aerospace Sciences,* vol. 47, no. 5, pp. 308–18,2011.

[5] Jameson, Antony. Aerodynamic Shape Optimization Using the Adjoint Method. *Lectures at the Von Karman Institute*, Brussels, 2003.

[6] Lambora, Annu, et al. 'Genetic Algorithm-A Literature Review'. *2019 International Conference on Machine Learning, Big Data, Cloud and Parallel Computing (COMITCon),* IEEE, pp. 380–84, 2019.

[7] Le Clainche, Soledad, et al. 'Improving Aircraft Performance Using Machine Learning: A Review'. *Aerospace Science and Technology*, pp. 108354, 2023.

[8] Alpaydin, Ethem. *Machine Learning*. 1st edition, MIT press, 2021.

[9] LeCun, Yann, et al. *Deep Learning*. Nature, vol. 521, no. 7553, pp. 436–44, May 2015.

[10]Kingma, Diederik P., and Max Welling. Auto-Encoding Variational Bayes. arXiv:1312.6114, arXiv, 10 Dec. 2022.

[11]Li, Jichao, et al. Machine Learning in Aerodynamic Shape Optimization. *Progress in Aerospace Sciences*, vol. 134, pp. 100849, 2022

[12]Chen, Wei, and Arun Ramamurthy. 'Deep Generative Model for Efficient 3D Airfoil Parameterization and Generation'. *AIAA SciTech 2021 Forum,* VIRTUAL EVENT, 2021.

[13]Li, Jichao, et al. 'Efficient Aerodynamic Shape Optimization with Deep-Learning-Based Geometric Filtering'. *AIAA Journal*, vol. 58, no. 10, pp. 4243–59, Oct. 2020.

[14]Yu, Boping, et al. 'An Improved Deep Convolutional Neural Network to Predict Airfoil Lift Coefficient'. *Proceedings of the International Conference on Aerospace System Science and Engineering 2019*, Toronto, Ontario, Canada, vol. 622, pp. 275–86, 2020.

[15]Zhang, Yao, et al. 'Application of Convolutional Neural Network to Predict Airfoil Lift Coefficient'. *2018 AIAA/ASCE/AHS/ASC Structures, Structural Dynamics, and Materials Conference*, Kissimmee, Florida, 2018.

[16]Bhatnagar, Saakaar, et al. 'Prediction of Aerodynamic Flow Fields Using Convolutional Neural Networks'. *Computational Mechanics*, vol. 64, no. 2, pp. 525–45, Aug. 2019.

[17]Thuerey, Nils, et al. 'Deep Learning Methods for Reynolds-Averaged Navier–Stokes Simulations of Airfoil Flows'. *AIAA Journal*, vol. 58, no. 1, pp. 25–36, Jan. 2020.

[18]Li, Runze, et al. 'Physically Interpretable Feature Learning of Supercritical Airfoils Based on Variational Autoencoders'. *AIAA Journal*, vol. 60, no. 11, pp. 6168–82, Nov. 2022.

[19]Du, Xiaosong, et al. 'A B-Spline-Based Generative Adversarial Network Model for Fast Interactive Airfoil Aerodynamic Optimization'. *AIAA Scitech 2020 Forum*, Orlando, FL, pp. 1 – 16, 2020.

[20]Barnhart, Samuel A., et al. 'Blown Wing Aerodynamic Coefficient Predictions Using Traditional Machine Learning and Data Science Approaches'. *AIAA Scitech 2021 Forum*, VIRTUAL EVENT, 2021.

[21]Raissi, M., et al. 'Physics-Informed Neural Networks: A Deep Learning Framework for Solving Forward and Inverse Problems Involving Nonlinear Partial Differential Equations'. *Journal of Computational Physics*, vol. 378, pp. 686–707, Feb. 2019.

[22]Karpatne, Anuj, et al. 'Theory-Guided Data Science: A New Paradigm for Scientific Discovery from Data'. *IEEE Transactions on Knowledge and Data Engineering*, vol. 29, no. 10, pp. 2318–31, 2017.

[23]Jia, Xiaowei, et al. 'Physics-Guided Machine Learning for Scientific Discovery: An Application in Simulating Lake Temperature Profiles'. *ACM/IMS Transactions on Data Science*, vol. 2, no. 3, pp. 1–26, Aug. 2021.

[24]Parish, Eric J., and Karthik Duraisamy. 'A Paradigm for Data-Driven Predictive Modeling Using Field Inversion and Machine Learning'. *Journal of Computational Physics*, vol. 305, pp. 758–74, 2016.

[25]Willard, Jared, et al. Integrating Scientific Knowledge with Machine Learning for Engineering and Environmental Systems. arXiv:2003.04919, arXiv, 13 Mar. 2022.

[26]Li, Runze, et al. 'Pressure Distribution Feature-Oriented Sampling for Statistical Analysis of Supercritical Airfoil Aerodynamics'. *Chinese Journal of Aeronautics,* vol. 35, no. 4, pp. 134–47, Apr. 2022.

[27]Menter, F. R. 'Two-Equation Eddy-Viscosity Turbulence Models for Engineering Applications'. AIAA Journal, vol. 32, no. 8, pp. 1598–605, Aug. 1994.

[28]Kulfan, Brenda M. 'Universal Parametric Geometry Representation Method'. *Journal of Aircraft*, vol. 45, no. 1, pp. 142–58, Jan. 2008.